Tribol Lett (2009) 36:233–238
DOI 10.1007/s11249-009-9478-7

ORIGINAL PAPER

# Characterization of Microscale Wear in a Polysilicon-Based MEMS Device Using AFM and PEEM–NEXAFS Spectromicroscopy

**D. S. Grierson · A. R. Konicek · G. E. Wabiszewski · A. V. Sumant · M. P. de Boer · A. D. Corwin · R. W. Carpick**

Received: 27 February 2009 / Accepted: 30 June 2009 / Published online: 14 July 2009


**Abstract** Mechanisms of microscale wear in silicon-based microelectromechanical systems (MEMS) are elucidated by studying a polysilicon nanotractor, a device specifically designed to conduct friction and wear tests under controlled conditions. Photoelectron emission microscopy (PEEM) was combined with near-edge X-ray absorption fine structure (NEXAFS) spectroscopy and atomic force microscopy (AFM) to quantitatively probe chemical changes and structural modification, respectively, in the wear track of the nanotractor. The ability of PEEM–NEXAFS to spatially map chemical variations in the near-surface region of samples at high lateral spatial resolution is unparalleled and therefore ideally suited for this study. The results show that it is possible to detect microscopic chemical changes using PEEM–NEXAFS, specifically, oxidation at the sliding interface of a MEMS device. We observe that wear induces oxidation of the polysilicon at the immediate contact interface, and the spectra are consistent with those from amorphous $SiO_2$. The oxidation is correlated with gouging and debris build-up in the wear track, as measured by AFM and scanning electron microscopy (SEM).

**Keywords** Microscale wear · Microelectromechanical systems (MEMS) · Nanotractor · Photoelectron emission microscopy (PEEM) · Atomic force microscopy (AFM)

D. S. Grierson (✉)
Department of Mechanical Engineering, University of Wisconsin-Madison, Madison, WI 53706, USA
e-mail: dsgrierson@wisc.edu

A. R. Konicek
Department of Physics and Astronomy, University of Pennsylvania, Philadelphia, PA 19104, USA

G. E. Wabiszewski · R. W. Carpick
Department of Mechanical Engineering and Applied Mechanics, University of Pennsylvania, Philadelphia, PA 19104, USA

A. V. Sumant
Center for Nanoscale Materials, Argonne National Laboratories, Argonne, IL 60439, USA

M. P. de Boer
MEMS Devices and Reliability Physics Department, Sandia National Laboratories, Albuquerque, NM 87185, USA

A. D. Corwin
MEMS Science and Technology Department, Sandia National Laboratories, Albuquerque, NM 87185, USA

## 1 Introduction

Micro-/nanoelectromechanical systems (MEMS/NEMS) promise to transform a number of industries by combining micro-/nanoelectronics with versatile micro-/nanofabrication technology. A multitude of MEMS technologies have been successfully fabricated and implemented, such as inertial and non-inertial sensors, actuators, relays, resonators, oscillators, filters, and switches [1]. However, because of their large surface-to-volume ratio, micro- and nanoscale devices designed to operate with sliding, contacting components are especially susceptible to premature failure due to adhesion, friction, and wear, thus hindering their commercialization [2, 3]. In order to overcome these tribological issues, we must understand the micro- and nanoscopic mechanisms by which surfaces become modified via interfacial interaction.

The tribological properties of MEMS devices made of polysilicon have been investigated and reported in several studies [4–10]. In this study we focus on understanding wear of the polysilicon-based MEMS nanotractor actuator.

Developed by de Boer and colleagues at Sandia National Laboratories, the nanotractor permits fundamental tribological studies of microscale mechanical contacts [11, 12]. The design and operation of the device is described in detail elsewhere [11]. In brief, the nanotractor consists of two planar friction clamps ($\sim$400 μm long, $\sim$150 μm wide) connected by an actuation plate (500 μm long and 50 μm wide) (Fig. 1a). Each friction clamp sits on two parallel $\sim$600 μm × 2 μm support rails that come into contact with the polysilicon substrate (henceforth referred to as the P0 layer) (Fig. 1b, c). Guide springs attached to the sides of the friction clamps provide a lateral force to the interface between the rails and the substrate, and voltages applied between the friction clamps and underlying electrodes provide normal forces. The nanotractor moves a "step" by alternately fixing the leading and trailing clamps while actuating the central actuation plate, which results in a sub-100-nm horizontal displacement of the device. The device can move hundreds of microns using these nanometer-sized steps.

The nanotractor can be used to measure both static and sliding friction coefficients, as well as interfacial adhesion [13], and was specifically designed to study the effect of applied load on friction and wear at the microscale. By virtue of the micromachining processes used to fabricate this microtribometer, the contacting surfaces can be roughened, oxidized, or coated with self-assembled monolayers (SAMs) to alter the strength of interfacial interactions. Thus, the structure and chemistry of the contacting surfaces can be tailored to conduct fundamental studies and to simulate the tribological conditions found in more complicated systems intended for commercial production.

Here, we present measurements of the morphology and chemistry of unworn and worn surfaces of a polysilicon MEMS device coated with a hydrophobic perfluorinated monolayer. Coating the polysilicon surfaces of the nanotractor with this film is known to improve wear performance [14], though premature device failure still occurs. Understanding the failure mechanism(s) of this microfabricated tribometer may guide future design of microscale tribosystems.

## 2 Experiment

Nanotractor devices, all contained on a single chip, were microfabricated at Sandia National Laboratory using the SUMMiT$^{TM}$ V process. A perfluorinated monolayer lubricant coating, (tridecafluoro-1,1,2,2-tetrahydrooctyl)tris(dimethylamino)-silane (FOTAS), was applied to the entire chip by a vapor deposition technique [15]. This technique allows FOTAS to conformally coat both contacting surfaces that comprise the sliding interface. Sliding tests were conducted on two different nanotractors in ambient air, at a relative humidity of 20–30%, with the specific intent to induce wear. Each test nominally consisted of moving a nanotractor $\sim$40 μm (i.e., to the left or to the right in Fig. 1a) in $\sim$50 nm steps, thereby deflecting the guide springs and applying a lateral force to the friction clamps. A fixed voltage of 20 V was then applied between the friction clamps and the clamp electrodes, which corresponds to a normal force of $\sim$47.2 μN on the load clamps. The device was then allowed to relax back to its initial position by lowering the normal force. Typical friction coefficients measured during these tests can vary from 0.3 to 4.0 depending on the sample preparation and the degree of wear [16]. This process was repeated in both directions for at least 500 complete cycles (i.e., an interval consisting of motion in both directions) for each device. After testing both nanotractors, the silicon chip was packaged and sealed to prevent contamination until the spectroscopic measurements were performed.

Photoelectron emission microscopy with near-edge x-ray absorption fine structure (PEEM–NEXAFS) spectroscopy measurements were performed ex-situ with the PEEM-II instrument at the Advanced Light Source at Lawrence Berkeley National Laboratory on Beamline 7.3.1.1. The clamps were removed from the silicon chip

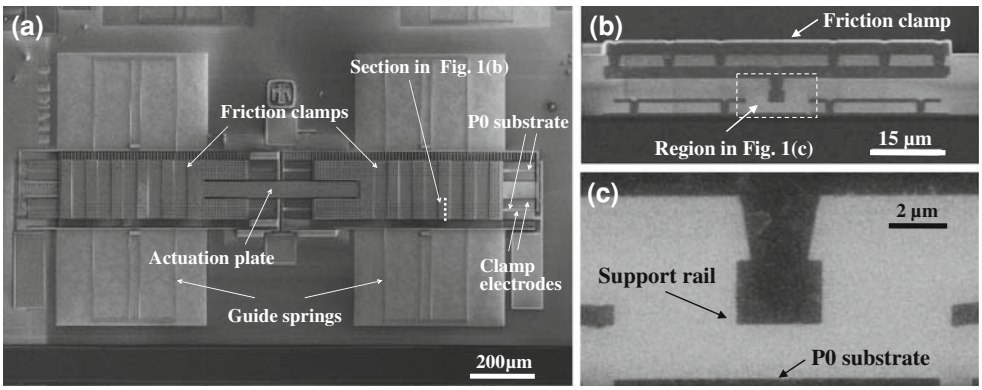


**Fig. 1** **a** SEM image of the polysilicon nanotractor MEMS device. **b** SEM cross-sectional view of a friction clamp and clamp electrodes. **c** SEM cross-sectional view of the support rail and P0 substrate

with adhesive tape prior to being inserted into the vacuum chamber. Electron emission images and x-ray absorption spectra were acquired from worn and unworn regions of the nanotractors at the C 1s, F 1s, and O 1s absorption edges. Unfortunately, this beamline could not accommodate Si spectroscopy. Because of the geometry of the nanotractor device and the 60° angle of incidence of the x-rays (from normal), special care had to be taken to properly align the sample to illuminate the P0 layer, which is ~4.5 μm deeper than the surrounding clamp electrodes. In addition, because of the susceptibility of FOTAS to radiation damage, we employed photon shutters to minimize the exposure of the surfaces to x-rays. All NEXAFS spectra were normalized by division to set the spectral intensity to 1.0 in the pre-edge region of each spectrum, which eliminated topographically-induced differences in the electron emission intensity. This allows spectra taken at different regions on the sample to be compared and ensures that relative peak heights correlate with atomic bonding concentrations. The sampling depth of the spectroscopy is less than 10 nm.

Atomic force microscopy (AFM) imaging was performed on the P0 layer with a Digital Instruments Multimode AFM with a Nanoscope IV controller. Areas of interest examined with the PEEM were imaged with AFM to correlate the topography and wear formation with the surface chemistry.

## 3 Results and Discussion

Figure 2 shows scanning electron microscopy (SEM) images of wear tracks on the P0 layer from two representative nanotractors which exhibited drastically different types of wear. The image in Fig. 2a is of a wear scar with a light amount of wear and minimal debris accumulation. The wear scar in Fig. 2b exhibits a high amount of wear, which is accompanied by significant debris formation in and around the wear track. These two images span the range of wear characteristics observed from these sets of tests and demonstrate the degree of surface modification and debris coverage encountered in these sliding conditions.

The 3D AFM image shown in Fig. 3 illustrates typical surface morphologies of worn regions (not shown in Fig. 2) and corresponds to an area analyzed with PEEM (discussed below). An average RMS roughness of ~4.4 nm was measured from images acquired on 120 locations of unworn P0-layer polysilicon, and an RMS roughness of ~2.5 nm was measured on an unworn location near the one depicted in Fig. 3. The unworn surface exhibits morphology due to the grain boundaries of the polysilicon as well as from roughness of the grains themselves. Multiple parallel trenches are observed along this entire track, and particles that lie directly on top of these trenches are found. These particles were deposited onto the track after the formation of the trenches. Two profiles are drawn on the

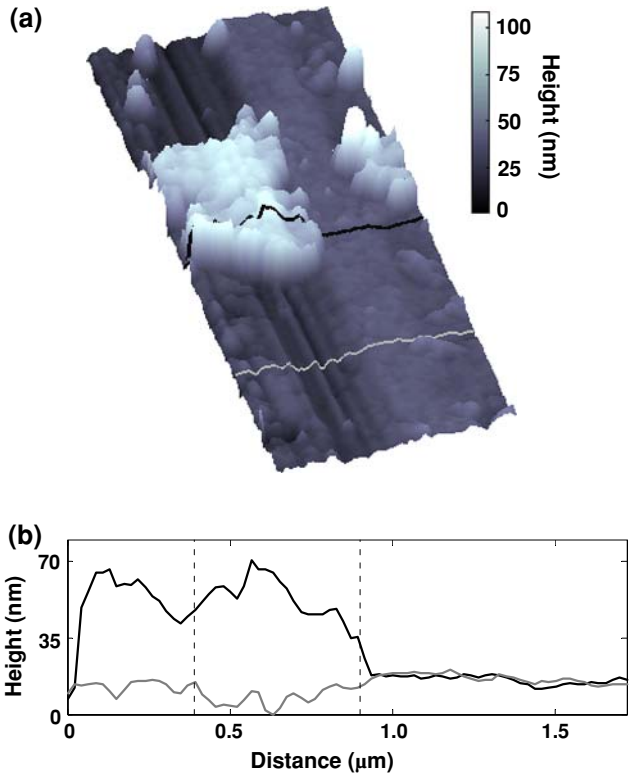


**Fig. 3** **a** 3D AFM topography image (~4.8 × ~1.7 μm$^2$) of a portion of a wear track partially covered with debris. **b** Line profiles of the debris particle and the gouged wear scar displayed in **a**

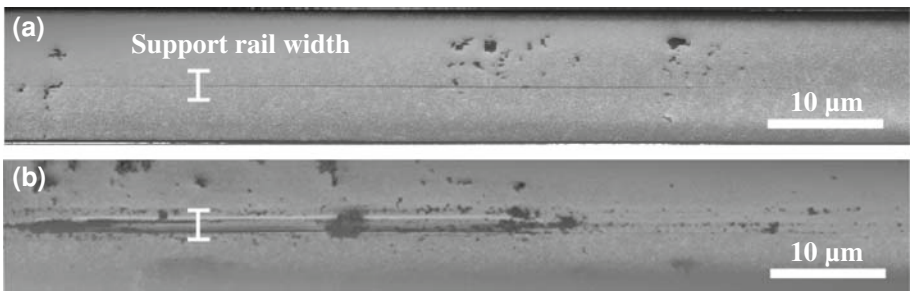


**Fig. 2** **a** SEM image of a lightly worn portion of the P0 layer. The width of the contacting support rail is labeled for each track. **b** SEM image of a wear scar exhibiting heavy wear and significant debris formation

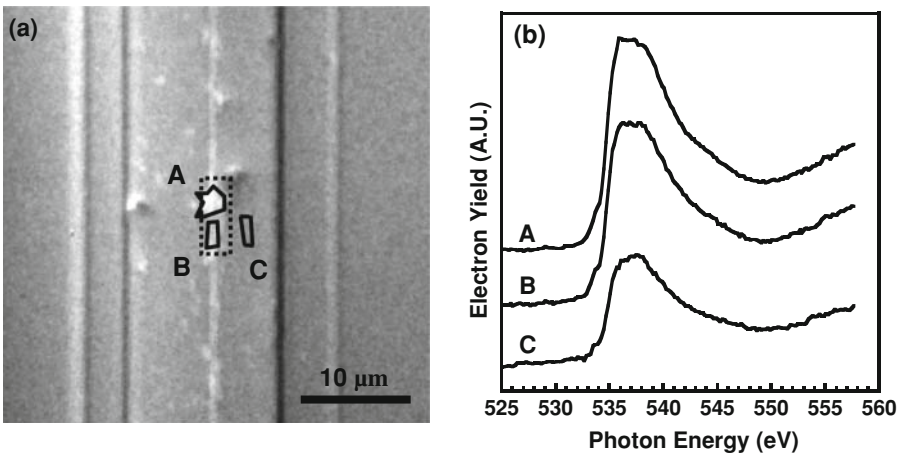


**Fig. 4** **a** PEEM image acquired with 530 eV x-rays of a portion of the P0 layer. The dashed rectangular region is the area depicted in Fig. 3a. **b** O 1s spectra, offset for clarity. Spectrum A is taken from a debris particle in the wear track, spectrum B is from a particle-free region of the wear track, and spectrum C is from an unworn region

3D AFM image orthogonal to the sliding direction, and the corresponding profiles are plotted in Fig. 3b. The lighter profile shows the relative depths of the wear scar gouges ($\sim$10 nm). The darker profile traverses a $\sim$70-nm high debris particle found over the wear scar (corresponding to region of interest (ROI) A in Fig. 4a). The average roughness of several hundred of these particles found on top of a similar nanotractor wear track was measured to be $\sim$1.3 nm RMS (measured over the entire wear track), whereas here the particle roughness is $\sim$5.8 nm (over a $1.0 \times 0.5$ $\mu m^2$ area). The remarkable average smoothness of these particles, which likely bear the load due to their height, demonstrates that they are subjected to a tribochemical polishing process. The high roughness of the debris particle in Fig. 3a indicates that this particle was likely deposited within the wear track near the end of the test. This is consistent with the idea that debris particles that are generated and subsequently worn within the sliding interface become smoother as the wear test progresses.

The PEEM–NEXAFS results are shown in Fig. 4. Figure 4a depicts a PEEM image acquired at 530 eV of a portion of the P0 layer viewed normal to the surface. The bright vertical line along the middle of the image is the wear scar. The other vertical lines arise from microfabricated changes in height of the substrate. The dashed rectangular region drawn in the PEEM image in Fig. 4a corresponds to the region imaged by AFM in Fig. 3a. Figure 4b is a plot of the oxygen (O 1s) spectra obtained from the highlighted ROIs drawn in Fig. 4a.

The most striking observation is that the O 1s spectra extracted from the debris and the wear track (spectra A and B, respectively) have similar shapes and intensities, and are substantially greater in intensity than the ROI unmodified by wear (spectrum C). This feature is indicative of the O 1s $\rightarrow \sigma^*$ transition and clearly demonstrates increased oxidation of the near-surface region of the worn interface, with the oxygen primarily bonded in a single-bonded state. Furthermore, none of the O 1s spectra exhibit a pre-edge feature at $\sim$532 eV. This absent pre-edge feature corresponds to the O 1s$\rightarrow \pi^*$ transition, and therefore, the lack of this feature demonstrates that no significant $\pi$-bonded oxygen, which would be expected for a double-bonded state, is present. These spectra have identical characteristics with those of amorphous $SiO_2$ found in the literature [17–19] and show no indication of crystalline Si–O bonding or oxides that deviate from the stoichiometry of $SiO_2$ [20]. NEXAFS spectra were also obtained at the carbon and fluorine edges (data not shown). In all cases, the C 1s and F 1s signals were weak everywhere (i.e., in both worn and unworn regions), indicating that their concentrations were at or below the detection threshold of the PEEM. There was no detectable difference in the C 1s and F 1s spectra between modified and unmodified regions for this wear track, although we have observed slight decreases in fluorine intensity in worn regions of other nanotractors, suggestive of removal of the FOTAS molecules.

The observed increase in the amount of Si–O bonding is in good general agreement with results found in the literature [21–23]. For example, Alsem et al. [23] used transmission electron microscopy (TEM) and energy dispersive x-ray (EDX) spectroscopy analyses to analyze debris particles formed in a polysilicon MEMS side-wall friction test device. Their TEM-EDX results confirmed that the debris particles and the wear track had higher oxygen contents than the surrounding unworn polysilicon, but they were unable to determine the exact oxidation state at the surface due to limitations of the EDX technique. However, they were able to estimate Si:O stoichiometry ratios of 34:66 and 80:20 in a debris particle and on a worn surface layer, respectively. From our spectroscopic results, we can conclude that oxidation of the debris and wear track due to wear in ambient laboratory conditions occurs solely in the form of $SiO_2$ bonding. The surface sensitivity and the sensitivity to chemical bonding states that PEEM–NEXAFS possesses allows us to advance our understanding of the nature of wear-induced oxidation of polysilicon by clearly

showing that only amorphous $SiO_2$ is formed on the immediate contact interface. Future study investigating the Si 1s and 2p edges will help inform the interpretation of the spectra further.

A more complete story of polysilicon wear emerges by combining PEEM spectroscopy and AFM topography. Based on previous studies of nanotractor friction and wear, we hypothesize that wear of the sliding interface begins as the FOTAS coating breaks down [14] within the contact zone and advances via moderate gouging, Si material removal (including the removal of individual grains as observed in the sidewall friction tests [23]), and debris formation within and around the contacting regions. Debris is mechanically polished and becomes oxidized to amorphous $SiO_2$, as does the wear scar. As elucidated by Flater et al., oxidized Si surfaces are known to exhibit higher friction [14], and therefore the wear scar and trapped oxidized debris may cause higher adhesion and friction, leading to further increase in wear. Device failure ultimately occurs at the time when the restoring force of the guide spring cannot exceed the lateral resistance produced by the $SiO_2$ debris formations and worn, oxidized surfaces.

## 4 Conclusions

Experiments using the nanotractor provide insight into the wear mechanisms for polycrystalline Si surfaces. PEEM–NEXAFS reveals that worn regions and debris formations have an increased amount of oxygen bonding, demonstrating that substantial oxidation in the form of amorphous $SiO_2$ takes place on mechanically modified polysilicon regions. AFM topography measurements confirm that the wear scar exhibits moderate gouging. More notably, debris, formed from gouging and from the removal of either entire grains or portions of grains from the substrate, can be trapped in the interface. The formation, smoothing, and oxidation of those particles, as well as the oxidation of the wear-scar gouges, characterize the wear process of the nanotractor.

By combining PEEM–NEXAFS with AFM, we are able to describe the wear processes that may lead to device failure from a combined chemical and mechanical perspective. This approach leads to an understanding of reliability and performance issues of a polysilicon MEMS device. Many of the concerns with MEMS/NEMS involving tribological contact can be addressed by applying these techniques to the materials and geometries currently employed in micro- and nanoscale wear studies.

**Acknowledgments** This study was partly funded by Air Force grant FA9550-08-1-0024, and partly by Sandia—a multiprogram laboratory operated by Sandia Corporation, a Lockheed Martin Company, for the United States Department of Energy's National Nuclear Security Administration under contract DE-AC04-94AL85000. The authors thank Dr. Scholl and Dr. Doran for their help with PEEM II at the Advanced Light Source (ALS). The ALS and use of the Center for Nanoscale Materials facility are supported by the DOE under Contract DE-AC02-05CH11231 and Contract DE-AC02-06CH11357, respectively.

## References

1. Maluf, N.: An introduction to microelectromechanical systems engineering. Meas. Sci. Technol. **13**, 229 (2002)
2. Romig Jr., A.D., Dugger, M.T., McWhorter, P.J.: Materials issues in microelectromechanical devices: science, engineering, manufacturability and reliability. Acta Mater. **51**, 5837 (2003)
3. de Boer, M.P., Mayer, T.M.: Tribology of MEMS. MRS Bull. **26**, 302 (2001)
4. Mehregany, M., Gabriel, K.J., Trimmer, W.S.N.: Integrated fabrication of polysilicon mechanisms. IEEE Trans. Electron. Dev. **35**, 719 (1988)
5. Yu-Chong, T., Muller, R.S.: IC-processed electrostatic synchronous micromotors. Sens. Actuators **20**, 49 (1989)
6. Lim, M.G., Chang, J.C., Schultz, D.P., Howe, R.T., White, R.M.: Polysilicon microstructures to characterize static friction. In: Proceedings of IEEE Micro Electro Mechanical Systems: An Investigation of Micro Structures, Sensors, Actuators, Machines, pp. 82–88 (1990)
7. Beerschwinger, U., et al.: A study of wear on MEMS contact morphologies. J. Micromech. Microeng. **4**, 95 (1994)
8. Sniegowski, J.J., Garcia, E.J.: Surface-micromachined gear trains driven by an on-chip electrostatic microengine. IEEE Electron Device Lett. **17**, 366 (1996)
9. Hall, A.C., et al.: Sidewall morphology of electroformed LIGA parts-implications for friction, adhesion, and wear control. J. Microelectromech. Syst. **14**, 326 (2005)
10. Alsem, D.H., et al.: Micron-scale friction and sliding wear of polycrystalline silicon thin structural films in ambient air. J. Microelectromech. Syst. **17**, 1144 (2008)
11. de Boer, M.P., et al.: High-performance surface-micromachined inchworm actuator. J. Microelectromech. Syst. **13**, 63 (2004)
12. Luck, D.L., de Boer, M.P., Ashurst, W.R. Baker, M.S.: Evidence for pre-sliding tangential deflections in MEMS friction. In: TRANSDUCERS '03. 12th International Conference on Solid-State Sensors, Actuators and Microsystems. Digest of Technical Papers (Cat. No.03TH8664), vol. 1, pp. 404–407 (2003)
13. Corwin, A.D., De Boer, M.P.: Effect of adhesion on dynamic and static friction in surface micromachining. Appl. Phys. Lett. **84**, 2451 (2004)
14. Flater, E.E., et al.: In situ wear studies of surface micromachined interfaces subject to controlled loading. Wear **260**, 580 (2006)
15. Hankins, M.G., Resnick, P.J., Clews, P.J., Mayer, T.M., Wheeler, D.R., Tanner, D.M., Plass, R.A.: Vapor deposition of amino-functionalized self-assembled monolayers on MEMS. In: Proceedings of SPIE—The International Society for Optical Engineering, vol. 4980, pp. 238–247 (2003)
16. Subhash, G., Corwin, A.D., Deboer, M.P.: Operational wear and friction in MEMS devices. American Society of Mechanical Engineers, Micro-Electro Mechanical Systems Division, MEMS, pp. 207–209 (2004)
17. Tsai, H.M., et al.: Enhancement of Si–O hybridization in low-temperature grown ultraviolet photo-oxidized $SiO_2$ film observed by X-ray absorption and photoemission spectroscopy. J. Appl. Phys. **103**, 013704 (2008)
18. Orignac, X., Vasconcelos, H.C., Almeida, R.M.: Structural study of $SiO_2$–$TiO_2$ sol–gel films by X-ray absorption and photoemission spectroscopies. J. Non-Cryst. Solids **217**, 155 (1997)

19. Grierson, D.S., et al.: Tribochemistry and material transfer for the ultrananocrystalline diamond-silicon nitride interface revealed by X-ray photoelectron emission spectromicroscopy. J. Vac. Sci. Technol. B **25**, 1700 (2007)
20. Gilbert, B., et al.: X-ray absorption spectroscopy of silicates for in situ, sub-micrometer mineral identification. Am. Mineral. **88**, 763 (2003)
21. Patton, S.T., Zabinski, J.S.: Failure mechanisms of a MEMS actuator in very high vacuum. Tribol. Int. **35**, 373 (2002)
22. Walraven, J.A., Headley, T.J., Campbell, A.N., Tanner, D.M.: Failure analysis of worn surface micromachined microengines. In: Proceedings of the SPIE—The International Society for Optical Engineering, vol. 3880, pp. 30–39 (1999)
23. Alsem, D.H., et al.: An electron microscopy study of wear in polysilicon microelectromechanical systems in ambient air. Thin Solid Films **515**, 3259 (2007)